

Atomistic model of reptation at polymer interfaces

D.G. Luchinsky^{1,2}, H. Hafiychuk¹, M. Barabash², V. Hafiychuk¹, K. Chaki³, H. Nitta³, T. Ozawa³, K. R. Wheeler⁴, P.V.E. McClintock²

¹SGT Inc., ARC, Moffett Field, California, USA, ²Department of Physics, Lancaster University, UK,

³Materials Science Section, Engineering Technology Division, JSOL Corp, JP, ⁴Ames Research Center, Moffett Field, California, USA

Abstract

We study a molecular dynamics model of a polymer-polymer interface for a polyetherimide/polycarbonate (PEI/PC) blend, including its thermodynamic properties, its chain reptation, and its corresponding welding characteristics. The strength of the sample is analyzed by measuring strain-stress curves in simulations of uni-axial elongation. The work is motivated by potential applications to 3D manufacturing in space.

Introduction

Understanding properties of polymer-polymer interfaces is a long-standing problem of fundamental and technological importance [1]. Polymer chains behavior such as reptation and entanglement determine the welding dynamics and strength in 3D printing [2]. The atomistic structure of polymers substantially influences these properties. However, earlier research was mostly focused either on bulk properties [3] or on coarse-grained models of interfaces [4].

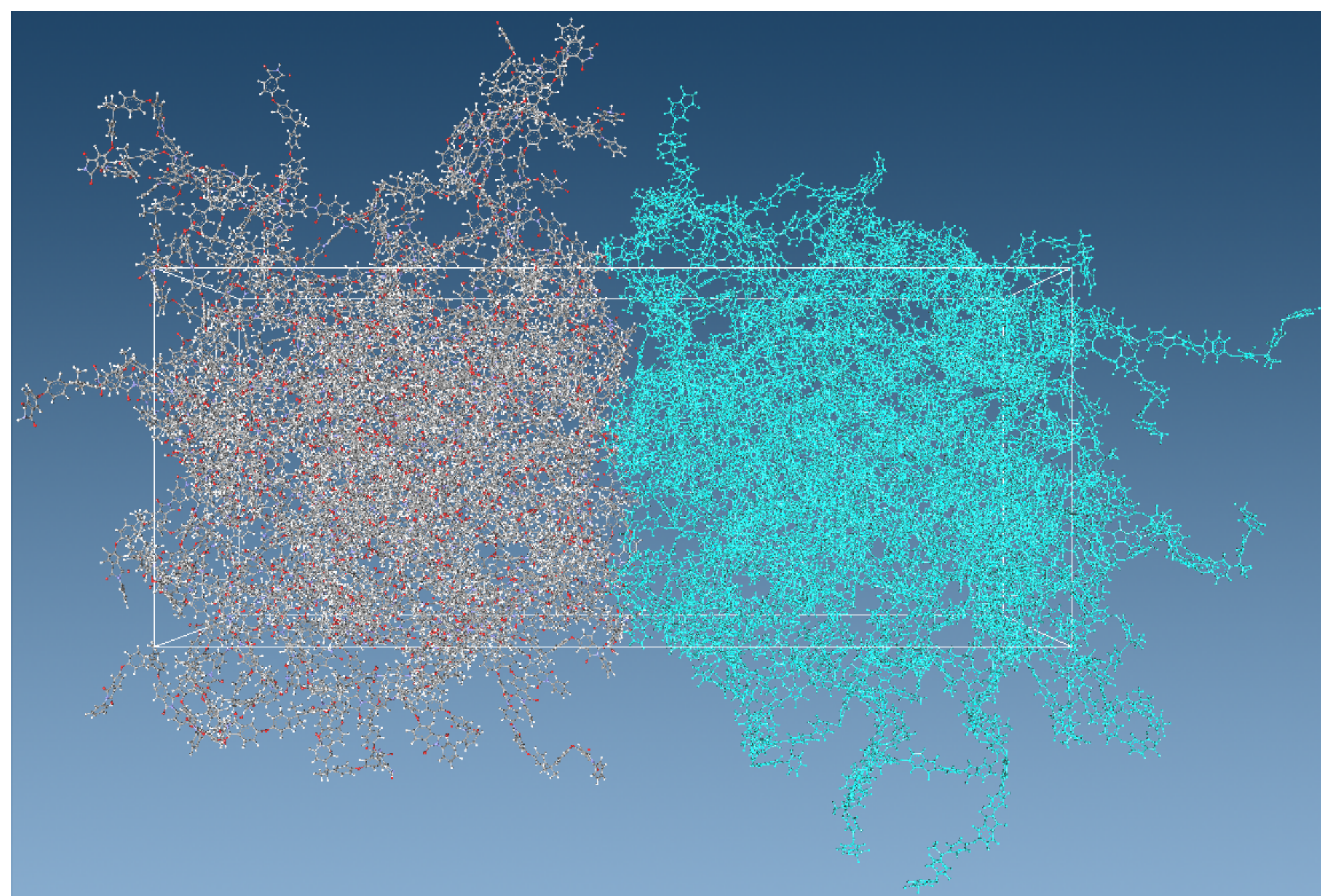


Figure 1: Two amorphous cells (gray and cyan) of PEI/PC polymer blend are combined in one chemical sample across an atomically flat interface.

Here we develop fully atomistic model of the polymer-polymer interface in PEI/PC blends. We assess MD capabilities in resolving polymer dynamics at polymer-polymer interfaces with atomic resolution and analyze thermal and mechanical properties of the blends in the presence of planar interface. We investigate the chains diffusion at the interface and the corresponding relaxation of the interface entanglement and non-bonding energy to the bulk state.

Model

We have prepared amorphous cells of these blends using the software package J-OCTA [5]. Cells were relaxed using the following procedure [5]: (i) equilibration in the NVE at a given temperature T_0 ; (ii) compression in the NPT Andersen-Nose-Hoover thermostat at T_0 and $P = 100$ MPa; (iii) additional equilibration in the NVE equilibration at T_0 ; (iv) relaxation in the NPT ensemble at T_0 and P_0 ; and (v) elimination of the translational component of the velocity in the NVT Nose-Hoover thermostat at T_0 and zero pressure. Each stage was computed during 100 ps with time step 1 fs. The temperature and the pressure during equilibration were $T_0 = 600$ K and $P_0 = 1$ atm (except for the 2-nd step, where $P = 100$ MPa.) The atomistically flat surfaces shown in Fig. 1 were prepared by moving polymer chains inside the cells and using LJ-wall. The parameters of the LJ-wall at the interface were: (i) cut-off ~ 10 Å; (ii) sigma ~ 5 Å; (iii) epsilon ~ 10 kJ/mol; and (iv) density ~ 20 g/cm³.

Validation

To validate the model we compared MD predictions with the following experimentally measured properties: (i) density ρ ; (ii) glass transition temperature T_g ; (iii) bulk modulus B ; (iv) coefficient of thermal expansion α_P ; (v) IR spectra and density of states $S(\nu)$; and (vi) specific heat capacity c_p .

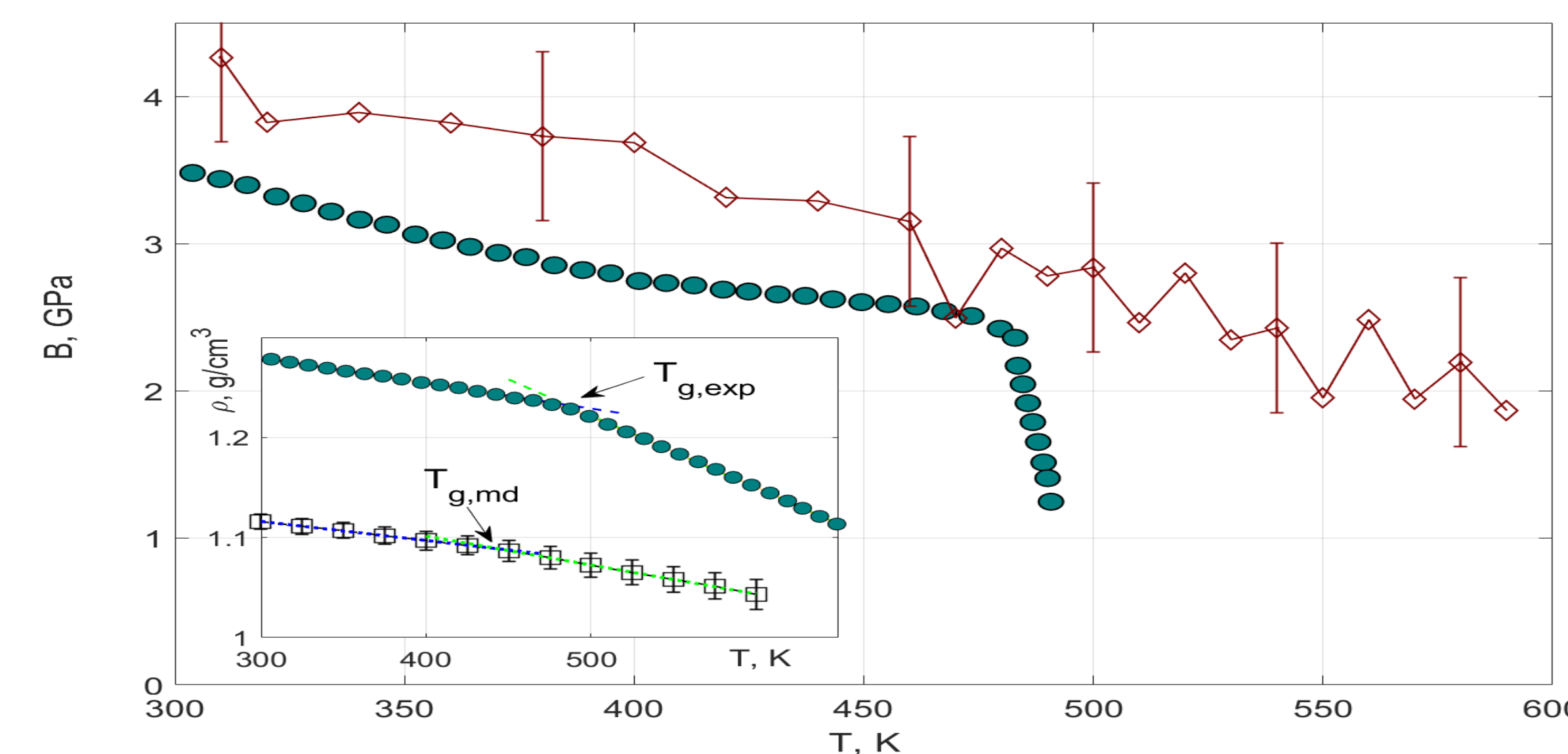


Figure 2: Bulk modulus B estimated using fluctuations (red open diamonds) in comparison with experimental data (teal circles). In the inset: density ρ vs T obtained in MD calculations as compared to the experimental data (teal circles). Arrows show the glass transition temperatures T_g obtained in experiment and simulations at the intersections of the straight lines corresponding to the linear fit of $\rho(T)$. Experimental data are given for ULTEM 1000 [6].

The 1-st example shows (see Fig. 2) the results of the bulk modulus (B) simulations in comparison with experimental data. The MD results were obtained using formula $B = V \langle \sigma_V^2 \rangle / k_B T$, where V is the volume, σ_V^2 is its variance, and k_B is the Boltzmann constant. Experimental data for $T < T_g$ were estimated using measured Young's modulus E and the equation $B = E/3(1 - 2\nu)$.

The good agreement of the developed model with experimental data paves the way to semi-quantitative predictions of the interface properties of the polymer blends considered.

of thermodynamic variables. The samples obtained after quenching and thermal cycling with different thickness of the welded layer were used for simulations of the strain-stress curves and shear viscosity. The profiles of the atomic densities on the two sides of the interface are shown in Fig. 3. It can be seen from the figure that the two samples are initially well separated, with the half-width of the gap at half bulk density ~ 5 Å. After ~ 0.5 ns the density at the interface has nearly reached its bulk value. After another 40 ns the density profiles stay almost the same with only the tails of the distributions extending to the other side by nearly 20 Å.

Shear viscosity

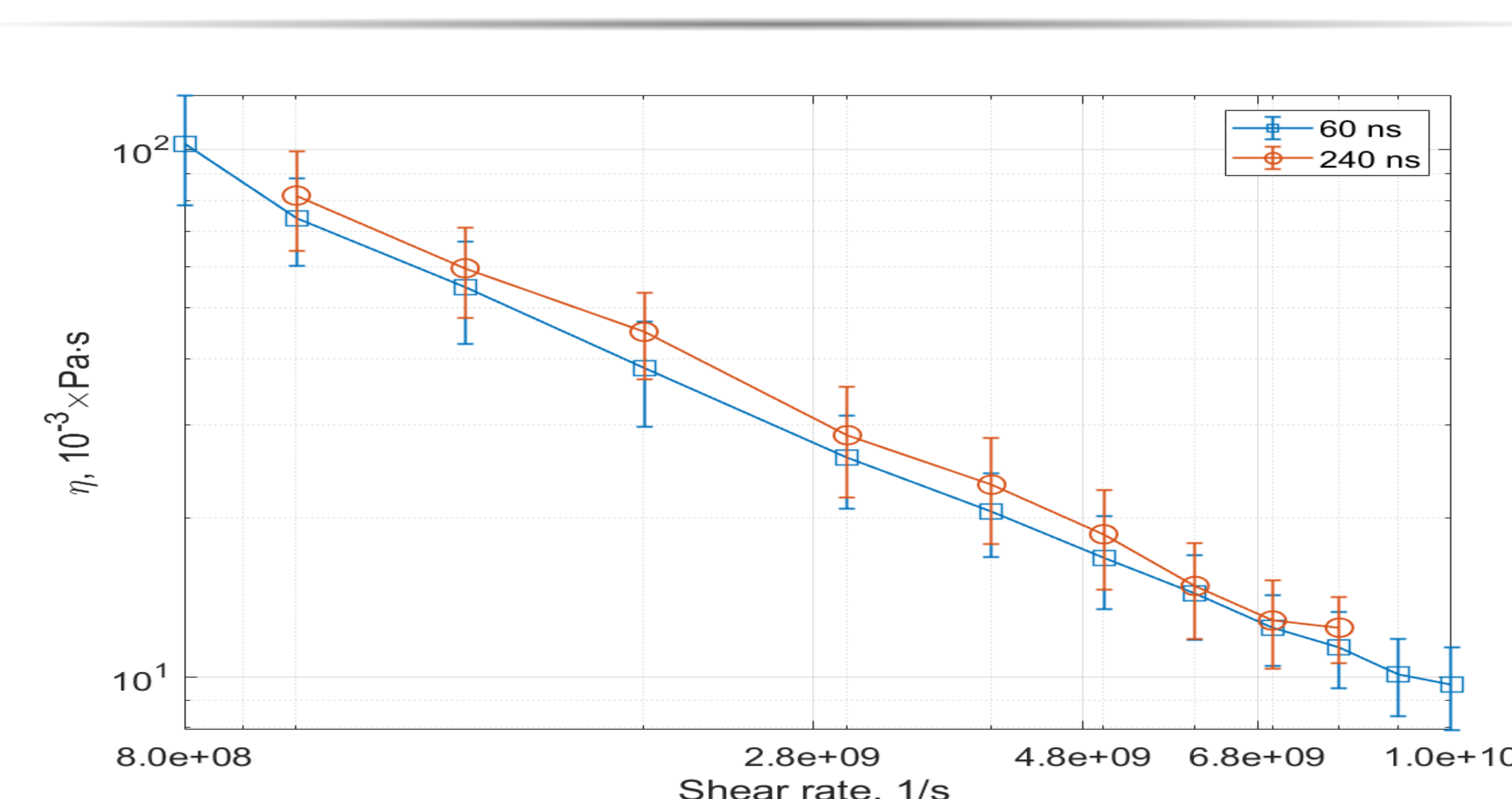


Figure 4: Shear viscosity as a function of shear rate for large system after 60 ns (blue square), 240 ns (brown circles) of healing and after thermal cycling (gray asterisk).

In the 2-nd example, the density ρ from the MD simulations is compared to the experimental data as a function of temperature (see the inset of Fig. 2). The linear fit of the $\rho(T)$ below and above the glass transition allows one to estimate T_g .

Diffusion of chains

To simulate welding dynamics the samples were allowed to equilibrate in the NPT ensemble that keeps pressure, temperature, and the total number of particles fixed (Note that the temperature at the interface of two filaments is nearly fixed during 300 ns used in MD simulations). At time instances 60 and 240 ns the sample was quenched to the room temperature. Additional thermal cycling between 300 and 600 K was used to analyze temperature dependence

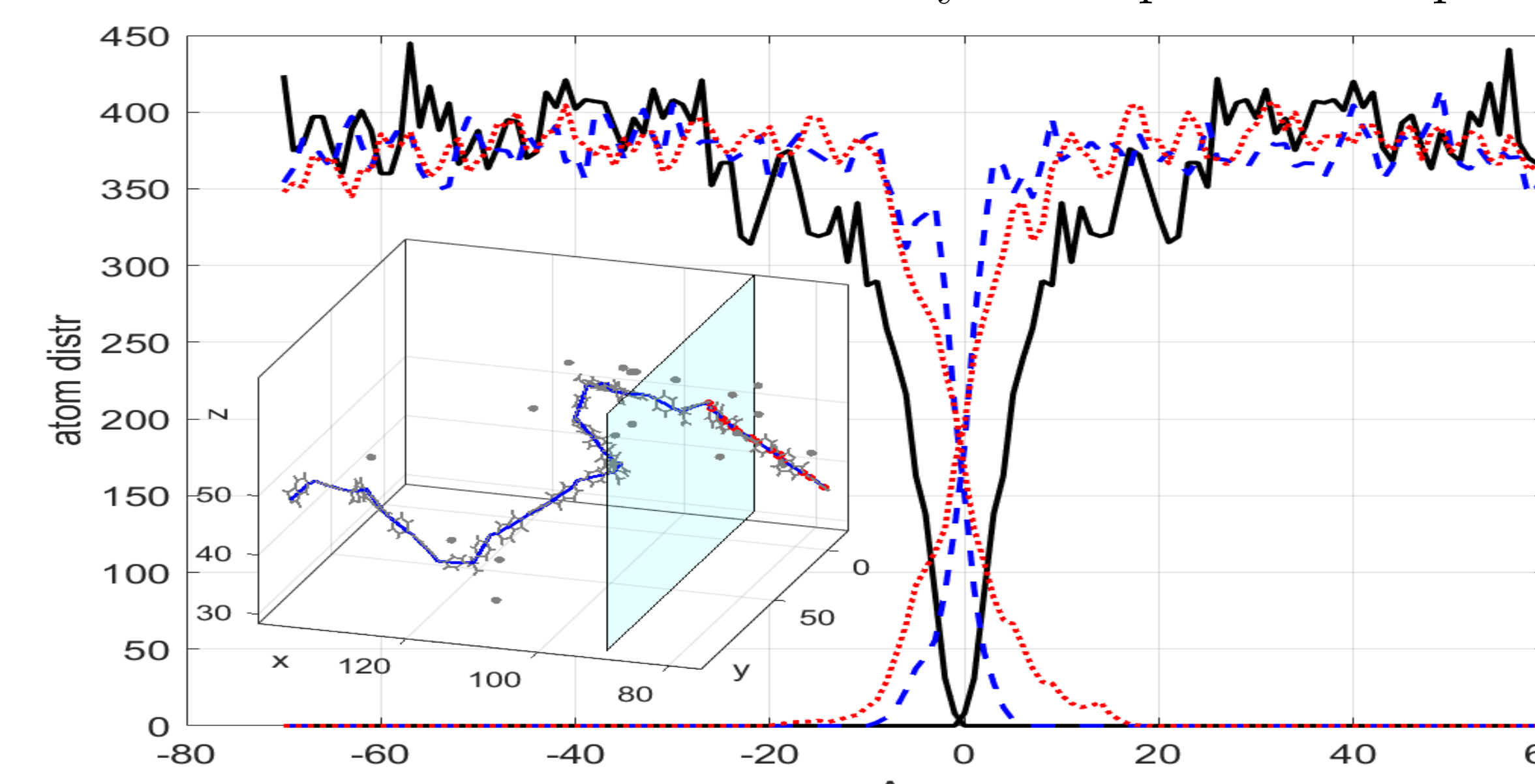


Figure 3: Atom density profiles of the polymers on both sides of the interface: (i) initial (black solid lines); (ii) at ~ 0.5 ns (blue dashed lines); (iii) at ~ 40 ns (red dashed lines). The inset shows example of a single chain reptation at the interface.

The shear deformation was applied in XY plane parallel to the interface plane of the sample. The results of simulation of shear deformation performed at welding times 60 ns and 240 ns are shown in Fig. 4. The dependence of η on the shear rate demonstrates characteristic shear thinning behavior, which can be clearly seen in log-log scale. Next, we observe that the shear viscosity calculated at 240 ns is shifted towards larger values as expected on theoretical grounds. However, this shift is consistent but is only weakly resolved (i.e. \propto error bars) for high shear rates used in MD simulations.

Strain-stress curves

The strain-stress curves obtained in the MD simulations for three different welding times are compared with the experimental curve in Fig. 5. The curves deviate from the experimental data due to the high elongation rate used in the MD simulations. However, it can be seen from the figure that both Young's modulus and the Yield strength increase as the thickness of welded layer increasing. We note that the calculations were performed under assumption of nominal Poisson's ratio $\nu = 0.36$. This assumption becomes increasingly inaccurate as the breaking of the sample is initiated at the interface. For this reason the strain-stress curves obtained in MD are shown by the dashed lines for the values of strain larger than 0.1.

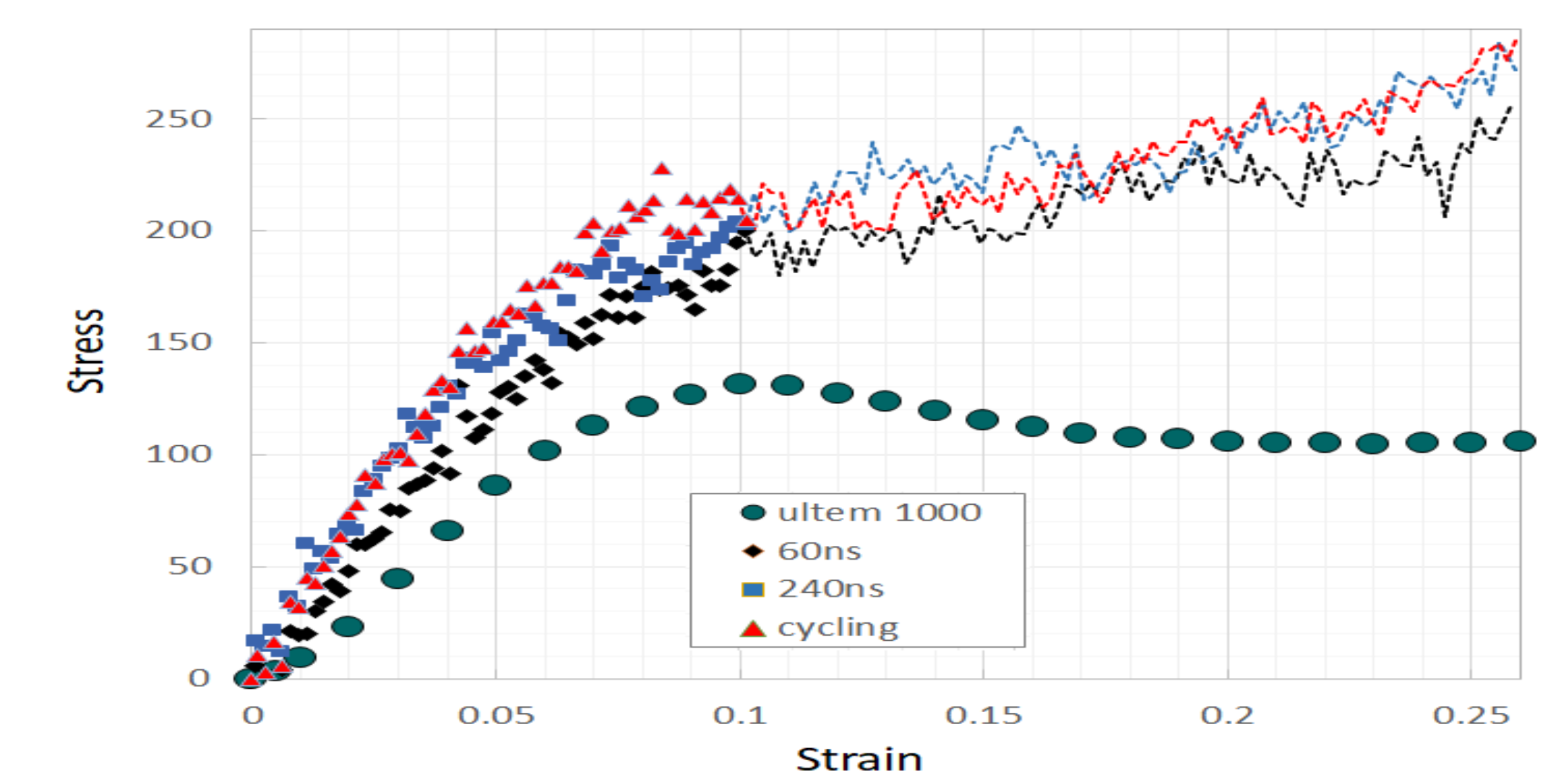


Figure 5: MD simulations of the strain-stress curves as a function of welding time: (i) 60 ns (diamonds); (ii) 240 ns squares; and (iii) after additional welding during temperature cycling (1200 ns). The experimental data obtained by ULTEM 1000 [6] are shown by teal shaded circles.

Conclusion

We developed a fully atomistic molecular dynamics model of the PEI/PC amorphous polymer blends with flat interface. The sample was welded for over 300 ns and quickly quenched to 300 K after 60 and 240 ns. The model was validated by comparison of the MD predictions with experimental data for the density, glass transition temperature, bulk modulus, and thermal expansion coefficient below T_g (where experimental data were available).

Two characteristic time scales of welding were observed: (i) fast diffusion ($t \lesssim 20$ ns) when chain's ends diffuse by filling in vacancies on both sides of the interface; and (ii) slow diffusion ($t \lesssim 300$ ns) when chain's ends slowly diffuse through the bulk material.

The analysis of the strain-stress curves as a function of time reveals the effect of the thickness of the welded layer on the strength of the interface. It was shown that both Young's modulus and the Yield strength increase as the thickness of welded layer increasing. Overall, the good agreement of the developed model with experimental data paves the way to semi-quantitative predictions of the interface properties of the polymer blends considered.

References

- [1] S. Prager and M. Tirrell, "The healing process at polymer-polymer interfaces", *The Journal of Chemical Physics*, 75(10):5194-5198, nov 1981.
- [2] Q. Sun, G.M. Rizvi, C.T. Bellehumeur, and P. Gu, "Effect of processing conditions on the bonding quality of FDM polymer filaments", *Rapid Prototyping Journal*, 14(2):72-80, 2008.
- [3] S. G. Falkovich, S. V. Lyulin, V. M. Nazarychev, S. V. Larin, A. A. Gurtovenko, N. V. Lukasheva, and A. V. Lyulin, "Influence of the electrostatic interactions on thermophysical properties of polyimides: Molecular-dynamics simulations", *Journal of Polymer Science Part B: Polymer Physics*, 52(9):640-646, feb 2014.
- [4] Ting Ge, Mark O. Robbins, Dvora Perahia, and Gary S. Grest, "Healing of polymer interfaces: Interfacial dynamics, entanglements, and strength", *Phys. Rev. E*, 90:012602, Jul 2014.
- [5] JSOL corp., *User's Manual, J-OCTA Overview, J-OCTA 4.0*, 2018.
- [6] Heat capacity, <https://www.protolabs.com/media/1014801/ultem-1000-im.pdf>, 2018.

Acknowledgements

We thank Gabriel Jost for the help in running simulations on Amazon Web Services. We thank Tracie Prayer for providing experimental data and guidance. The research was supported by NASA STMD/GCD/LSM grant in Space Manufacturing and by a Leverhulme Trust Research Project Grant RPG-2017-134.